Title	Entropic potential field formed for a linear-motor protein near a filament: Statistical-mechanical analyses using simple models.
Author(s)	Amano, Ken-Ichi; Yoshidome, Takashi; Iwaki, Mitsuhiro; Suzuki, Makoto; Kinoshita, Masahiro
Citation	The Journal of chemical physics (2010), 133(4)
Issue Date	2010-07-28
URL	http://hdl.handle.net/2433/128760
Right	© 2010 American Institute of Physics
Type	Journal Article
Textversion	publisher

Entropic potential field formed for a linear-motor protein near a filament: Statistical-mechanical analyses using simple models

Ken-ichi Amano,[1] Takashi Yoshidome,[2] Mitsuhiro Iwaki,[3] Makoto Suzuki,[4] and Masahiro Kinoshita[2,a)]
[1]*Graduate School of Energy Science, Kyoto University, Uji, Kyoto 611-0011, Japan*
[2]*Institute of Advanced Energy, Kyoto University, Uji, Kyoto 611-0011, Japan*
[3]*Graduate School of Medicine, Osaka University, Suita, Osaka 565-0871, Japan*
[4]*Department of Materials Processing, Graduate School of Engineering, Tohoku University, Aoba-ku, Sendai 980-8579, Japan*

(Received 5 May 2010; accepted 17 June 2010; published online 27 July 2010)

We report a new progress in elucidating the mechanism of the unidirectional movement of a linear-motor protein (e.g., myosin) along a filament (e.g., F-actin). The basic concept emphasized here is that a potential field is entropically formed for the protein on the filament immersed in solvent due to the effect of the translational displacement of solvent molecules. The entropic potential field is strongly dependent on geometric features of the protein and the filament, their overall shapes as well as details of the polyatomic structures. The features and the corresponding field are judiciously adjusted by the binding of adenosine triphosphate (ATP) to the protein, hydrolysis of ATP into adenosine diphosphate (ADP)+Pi, and release of Pi and ADP. As the first step, we propose the following physical picture: The potential field formed along the filament for the protein without the binding of ATP or ADP+Pi to it is largely different from that for the protein with the binding, and the directed movement is realized by repeated switches from one of the fields to the other. To illustrate the picture, we analyze the spatial distribution of the entropic potential between a large solute and a large body using the three-dimensional integral equation theory. The solute is modeled as a large hard sphere. Two model filaments are considered as the body: model 1 is a set of one-dimensionally connected large hard spheres and model 2 is a double helical structure formed by two sets of connected large hard spheres. The solute and the filament are immersed in small hard spheres forming the solvent. The major findings are as follows. The solute is strongly confined within a narrow space in contact with the filament. Within the space there are locations with sharply deep local potential minima along the filament, and the distance between two adjacent locations is equal to the diameter of the large spheres constituting the filament. The potential minima form a ringlike domain in model 1 while they form a pointlike one in model 2. We then examine the effects of geometric features of the solute on the amplitudes and asymmetry of the entropic potential field acting on the solute along the filament. A large aspherical solute with a cleft near the solute-filament interface, which mimics the myosin motor domain, is considered in the examination. Thus, the two fields in our physical picture described above are qualitatively reproduced. The factors to be taken into account in further studies are also discussed. © *2010 American Institute of Physics*. [doi:10.1063/1.3462279]

I. INTRODUCTION

Modern biology has shown that the so-called motor proteins play crucially important roles in a number of biological, motile processes. Both rotatory- and linear-motor proteins are known to exist. The latter is considered in the present article. Three different families of linear-motor proteins have been identified and well studied at the single-molecule level: kinesins,[1] dyneins,[2] and myosins.[3] The linear-motor proteins share the following common features: They move in one direction along the filaments, similar in function to railway tracks, which possess periodic structures. They repeat the biochemical cycle comprising the binding of adenosine triphosphate (ATP) to the motor domain (i.e., the head) of the protein, hydrolysis of ATP into adenosine diphosphate (ADP)+Pi, and release of Pi and ADP.[4–8] Many of them have two-headed structures. However, it has been found that even a single-headed kinesin[9] or a single myosin head,[8,10,4,11,12] [i.e., myosin subfragment 1 (S1)] exhibits the unidirectional movement. Hence, the two-headed structures are not essential in the unidirectional movement, and the fundamental physics can be extracted by means of studies for a single linear-motor protein head. Although the mechanism of the unidirectional movement has been investigated extensively, it still remains rather mysterious. A commonly accepted hypothesis is the lever-arm model.[13] Models based on a biased Brownian motion in a potential field formed for the protein have also been described.[8,10,4,11,12,14–16] There is an interesting study[17] arguing that the Brownian motion is spa-

a)Author to whom correspondence should be addressed. Electronic mail: kinoshit@iae.kyoto-u.ac.jp.

tially asymmetrical for a mesoscopic particle embedded in a fluid if the particle is not in equilibrium with the fluid and its shape is nonspherical. In the present article, we are concerned with a physical origin of the potential field for the biased Brownian motion.

A typical example of the linear-motor proteins is myosin moving along filamentous actin (F-actin). F-actin possesses a double helical structure formed by two sets of connected G-actin molecules.[18,19] On the basis of the results of experimental studies,[4–8] it is inferred that the following cycle is repeated: (1) Myosin (a head of myosin) is strongly bound to a rigor binding site of F-actin in the absence of the ATP or ADP binding to myosin; (2) upon the ATP binding to myosin, myosin is only weakly bound to F-actin, and the directed movement of myosin occurs by a biased Brownian motion; (3) the hydrolysis of ATP into ADP+Pi occurs in the course of the Brownian motion; (4) after the release of Pi, myosin is bound to another rigor binding site of F-actin moderately strongly; (5) the binding becomes strong after the release of ADP. It has been argued that the electrostatic attractive interaction plays an essential role in the rigor binding of myosin to F-actin.[16,20] However, this argument conflicts with the experimental data that the binding of myosin to F-actin accompanies positive changes in entropy and enthalpy[21–23] (i.e., the binding is entropically driven). In our opinion, the direct interaction (or the screened electrostatic interaction) between myosin and F-actin has been treated as the dominant factor while the roles of water have caught much less attention. Here we suggest a completely different concept that the unidirectional movement of the linear-motor proteins is controlled primarily by the entropic effect originating from the translational displacement of water molecules.

The entropic excluded-volume effect plays critical roles in biological systems.[24–26] Many biological processes are controlled by the interactions between macromolecules and by those of macromolecules with macromolecular complexes. The macromolecules and complexes generate excluded volumes for smaller particles forming the solvent (i.e., volumes of the spaces which the centers of solvent particles cannot enter). When the macromolecules approach each other, for instance, the excluded volumes overlap, leading to an increase in the total volume available to the translational displacement of solvent particles. That is, the number of accessible configurations of the solvent that coexist with the macromolecules in the system increases and a corresponding entropy gain occurs. Thus, an attractive force is induced between macromolecules at small separations.[27,28] The entropic forces are largely influenced by the overall shape of macromolecules and macromolecular complexes as well as their detailed polyatomic structures. It should be emphasized that the entropic effect is *omnipresent*.

We believe that the most important concept relevant to the behavior of a linear-motor protein is the following: For a large sphere on a wall, geometric features of the wall induce entropic force (or potential) acting on the large sphere in a specific direction *along* the wall.[24,25,29–31] For example, the large sphere is locally repelled from a step edge,[32] attracted to a corner, and moved from a convex surface to a concave one (see Fig. 1). Further, it is difficult for the large sphere to get well separated from the wall. To elucidate the concept, theoretical studies dealing with large bodies with simple geometries immersed in small particles have been reported in literature.[24,25,29–31] In these studies, the hard-body models are employed for the large bodies and small particles. In the hard-body models, all the accessible system configurations share the same energy, and the system behavior is purely entropic in origin: They allow us to investigate the entropic effect *exclusively*. In biological systems, the solvent is water characterized by hydrogen bonds. However, in the entropic gain upon the solute contact and related processes, the translational entropy predominates over the rotational entropy.[25,26,33–35] The basic physics of the entropic effect considered here can be captured by modeling water as hard spheres in many cases, as long as the diameter and number density are set at the values of water.[25,26] We note that due to the hydrogen-bonding water can exist as a dense liquid despite its quite a small molecular size, leading to an exceptionally large entropic effect.

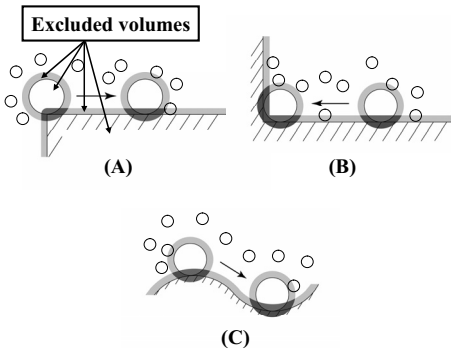

FIG. 1. Entropic force (or potential) acting on a large sphere. It reflects geometric features of the wall. The large sphere and the wall generate the excluded volumes. The large sphere tends to be moved so that the overlap of the excluded volumes marked in black can increase. The large sphere is locally repelled from a step edge (a), attracted to a corner (b), and moved from a convex surface to a concave one (c). If the large sphere is well separated from the wall, there is no overlap of the excluded volumes, which is entropically unfavorable for the solvent.

A problem revealed by earlier works[24,25,29–31,36–47] is the following. The effect of the density structure of small spheres near the big bodies is essential, making the entropic interaction rather complicated. Between large spheres, for example, the induced interaction exhibits a great variation with the period which is close to the diameter of small spheres, and attractive and repulsive regions appear alternately. The details of the entropic effect are strongly dependent on geometric characteristics of the particular system considered.[24,29,30,47] These properties cannot be reproduced by the simple Asakura–Oosawa theory,[27,28] which gives only a much shorter-ranged, monotonically changing attractive force. Thus, it is challenging to investigate the entropic effect for a new system using an elaborate statistical-mechanical theory.

In the conventional view,[48] only the water in the close vicinity of the solute surface is considered, and the water-entropy effect is argued primarily in terms of the solute-water orientational correlation, changed hydrogen-bonding network of water, and restriction of the rotational freedom of water molecules. We emphasize that the water-entropy effect

considered in the present study, which reaches a far larger length scale,[25,26,34,49] is substantially different from the conventionally argued one and much larger.[34]

We have a new physical picture of the unidirectional movement of a linear-motor protein along a filament. A potential field is formed for the protein on the filament due to the water-entropy effect. The entropic potential field is strongly dependent on geometric features of the protein and the filament, their overall shapes as well as details of the polyatomic structures. The features and the corresponding field are judiciously adjusted by the binding of ATP to the protein, hydrolysis of ATP into ADP+Pi, and release of Pi and ADP. Although the picture should be somewhat complicated in its details, in the present article we propose the following outline as the first step: The potential field formed along the filament for the protein without the binding of ATP or ADP+Pi to it is largely different from that for the protein with the binding, and the directed movement is realized by repeated switches from one of the fields to the other. To illustrate it, we report the results of theoretical analyses performed for actomyosin (i.e., myosin and F-actin) as a typical example. A single myosin head (S1) is considered. The spatial distribution of the entropic potential between a large solute and a large body is calculated using the three-dimensional (3D) integral equation theory.[24,30,44,47,50–52] The solute is modeled as a large hard sphere. Two model filaments are considered as the body: Model 1 is a set of one-dimensionally connected large hard spheres and model 2 is a double helical structure formed by two sets of connected large hard spheres. The solute and the filament are immersed in small hard spheres forming the solvent. It is found that the solute is strongly confined within a narrow space in contact with the filament. Within the space there are locations with sharply deep local potential minima along the filament. The distance between two adjacent locations is equal to the diameter of the large spheres constituting the filament. The results from models 1 and 2 are compared to discuss the role of the double helical structure. Further, by considering a large aspherical solute with a cleft near the solute-filament interface, we show that geometric features of the solute have large effects on the amplitudes and asymmetry of the entropic potential field acting on the solute along the filament.

In the present study, we concentrate on the entropic component of the solvation of solutes. Further, in our model the effects due to the specific protein-water interactions (e.g., electrostatic and van der Waals interactions) are not taken into account. It should be noted, however, that the entropic potential field is much more influenced by geometric characteristics of the proteins as shown in our earlier works.[25,26,53] By "geometric characteristics" we mean overall shapes as well as polyatomic structures. We investigate the effects of overall shapes as the first step. Those of polyatomic structures including their flexibility are to be examined in a future work.

The rest of the present article is organized as follows. The preliminary physical picture of the unidirectional movement of myosin along F-actin is described in Sec. II. As a matter of fact, the picture has been developed on the basis of not only the experimentally available information but also the results of our theoretical calculations presented in Sec. IV. However, we believe that it is more appealing to describe the picture first. In Sec. II, the behavior of myosin expected from the picture is compared with the experimental result by single-molecular measurements for S1.[8,10,4,11,12] The model and theory employed are explained in Sec. III. We examine the calculation results from the two different models of the filament in Sec. IV. The effects of geometric features of the large solute are also argued in the light of the results of further model calculations. The basic characteristics of the two different potential fields in our physical picture are qualitatively reproduced. Section V concludes the article with final discussion and summary.

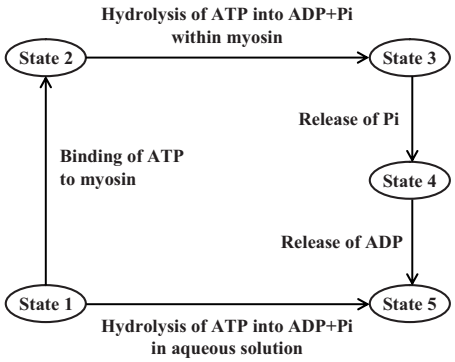

FIG. 2. One cycle comprising state 1→state 2→state 3→state 4→state 5.

II. PHYSICAL PICTURE FOR MECHANISM OF UNIDIRECTIONAL MOVEMENT OF MYOSIN ALONG F-ACTIN

A. Summary of experimental observations

Clues to the mechanism of the unidirectional movement of myosin (S1) along F-actin are in the following experimental observations. If there is no ATP in aqueous solution, myosin keeps binding to a rigor binding site of F-actin and does not move.[54–56] In the presence of ATP, the cycle illustrated in Fig. 2 is repeated:[4–8] the binding of ATP to myosin, hydrolysis of ATP into ADP+Pi, release of Pi, and release of ADP. In each cycle comprising the four changes, the system free energy is lowered by the free-energy change arising from the hydrolysis of ATP in aqueous solution, state 1→state 5. Geometric features (i.e., overall shape and details of the polyatomic structure) of myosin without the ATP or ADP+Pi binding to it in states 1, 4, and 5 are largely different from those of myosin with the binding in states 2 and 3.[4–8] Myosin becomes only weakly bound to F-actin upon the ATP binding,[22,23] allowing a biased Brownian motion. The motion continues until myosin is bound to another rigor binding site after the release of Pi. During the motion, myosin steps back and forth stochastically along F-actin. According to the experimental result by single-molecular measurements for S1,[8,10,4,11,12] the typical step size is ~5.3 nm that is almost equal to the size of G-actin, 5.5 nm. In one cycle mentioned above, myosin makes a movement consisting of 1–5 steps

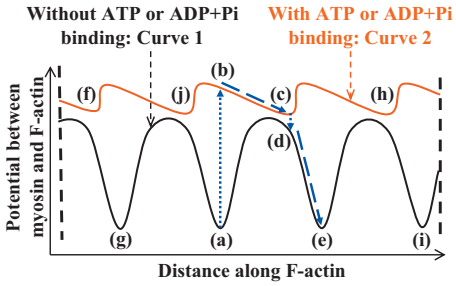

FIG. 3. Our preliminary physical picture of directed movement of myosin along F-actin.

(1 step with the highest probability and ~2.5 steps on the average). In one cycle myosin moves by the distance which lies in the range from 5 to 30 nm. Last, it is worthwhile to emphasize that the binding of myosin to F-actin is entropically driven.[21–23]

B. Two principal entropic potential curves

The outline of our physical picture, which is based on the experimental observations and on the results of our theoretical calculations presented in Sec. IV, is illustrated in Fig. 3. We concentrate on the entropic effect originating from the translational displacement of water molecules. Myosin, which is entropically confined within a narrow space in contact with F-actin, feels the entropic potential field along F-actin. Since the structure of F-actin is periodic, the field is also periodic. The field is strongly dependent on geometric features of myosin, and it exhibits a large change upon the ATP binding to myosin. The fields felt by myosin without the ATP or ADP+Pi binding to it and by myosin with the binding correspond to curve 1 drawn in black and to curve 2 drawn in red, respectively. The two oscillatory curves should be fairly complicated, but they are simplified in the illustration. The most important feature required for curve 1 is that it has locations with sharply deep potential minima corresponding to the rigor binding sites of F-actin. It is not essential whether curve 1 is asymmetrical or not for each period. Since at least one of the curves should be asymmetrical, curve 2 is asymmetrical if curve 1 is assumed to be symmetrical as shown in Fig. 3. The amplitudes of curve 2 are considerably smaller than those of curve 1. In both curves 1 and 2, the distance between two adjacent local potential minima is equal to the size of G-actin, 5.5 nm.

In our picture, the unidirectional movement of myosin along F-actin is reached by the following three principal steps:

(I) Myosin without the ATP or ADP (i.e., nucleotide) binding to it is highly stabilized on a location with the sharply deep local potential minimum of curve 1 [see (a) in Fig. 3]: Myosin can hardly move.

(II) The geometric features of myosin are changed by the ATP binding, which leads to the change in the potential field from curve 1 to curve 2. Myosin is no more stabilized on the location in step I [see (b)]. Along the negative slope of curve 2 [(b)→(c)], myosin moves to a new location with the local potential minimum [see (c)].

(III) The hydrolysis of ATP and the release of Pi occur. The original geometric features of myosin are recovered and the potential field returns to curve 1. Myosin is no more stabilized on the location in step II [see (d)]. Along the negative slope of curve 1 [(d)→(e)], myosin moves to the nearest location with the deep local potential minimum [see (e)]. (The release of ADP occurs before the ATP binding to myosin.)

Myosin tends to be trapped on a location with the local potential minimum of curve 2. However, sufficiently small amplitudes of curve 2 allow a biased Brownian motion of myosin, and it sometimes exhibits different movements: It moves backward [(b)→(f)→(g)], it moves forward to a farther location with the local potential minimum [e.g., (b)→(c)→(h)→(i)], or it makes essentially no movement [(b)→(j)→(a)]. The most probable route should be (a)→(b)→(c)→(d)→(e). Thus, the unidirectional movement of myosin is certainly realized. However, myosin appears to move only by 5.5 nm on the average in one cycle. This behavior is not quite consistent with the experimental result that in one cycle myosin moves by the distance which lies in the range from 5 to 30 nm.[8,10,4,11,12] The consistency is obtained if, for example, a component such as $-ax$ (x is the distance along F-actin and $a>0$ is the slope) is added to curve 2. Such a component could effectively be incorporated by accounting for the details neglected in the present picture as discussed in Sec. II C.

Aqueous solution consisting of water molecules, ATP, Pi, and ADP is referred to as the solvent. As explained in Sec. III B, an entropic potential of curve 1 represents "the free energy of the solvent in the case where myosin without the ATP or ADP+Pi binding is on a location of F-actin" *relative to* "the free energy of the solvent in the case where myosin without the ATP or ADP+Pi binding is infinitely separated from F-actin." Likewise, an entropic potential of curve 2 represents "the free energy of the solvent in the case where myosin with the ATP or ADP+Pi binding is on a location of F-actin" *relative to* "the free energy of the solvent in the case where myosin with the ATP or ADP+Pi binding is infinitely separated from F-actin." We emphasize that curves 1 and 2 have different reference values of the solvent free energy: The reference value in curve 2 is lower than that in curve 1 by the free-energy change upon the ATP or ADP+Pi binding to myosin whose absolute value should be larger than "the entropic potential at (b)" minus "the entropic potential at (a)." Therefore, the actual free energy of the solvent *decreases* upon the ATP binding to myosin. Further, the free energy of the solvent exhibits small but significant decreases in each of the succeeding changes illustrated in Fig. 2: It is in the order state 2 > state 3 > state 4 > state 5. It follows that the reference value of the solvent free energy continues to decrease. Thus, the curve of the actual free energy of the solvent continues to exhibit a parallel, downward shift. When myosin moves from (a) to another location such as (e), (g), or (i) in one cycle, the system free energy is lowered by the free-energy change arising from the hydrolysis of ATP in

aqueous solution, state 1 → state 5. However, the unidirectional movement is not influenced by the changes in the reference value of the solvent free energy because it is governed by the derivative of the potential curve with respect to x multiplied by −1 (i.e., the entropic force in the x-direction).

C. Further discussion

As mentioned in Sec. II B, the behavior of myosin in the physical picture is not quite consistent with the experimental result that in one cycle myosin can move by the distance which is substantially longer than 5.5 nm.[8,10,4,11,12] This problem could be solved if we consider that geometric features of myosin and the potential curve undergo small but significant changes as the hydrolysis of ATP proceeds (state 2 → state 3) and upon the release of ADP (state 4 → state 5). In a strict sense, myosin with the ATP binding in state 2, myosin with the ADP+Pi binding in state 3, and myosin with the ADP binding in state 4 are more or less different from one another in terms of geometric features[5,6,57,58] and the potential field felt by myosin. It follows that at least four curves should be considered. Moreover, any change from one curve to the next one occurs not abruptly but gradually. There is one more factor which can be substantial: Geometric features of the portion of F-actin near myosin are different from those of the rest and variable during each cycle.[59]

The biased Brownian motion is described by the entropic force (i.e., the derivative of the entropic potential with respect to x multiplied by −1). When the force is positive, myosin is driven to move in the positive direction along the x-axis. Myosin can move by the distance which is substantially longer than 5.5 nm if the following is satisfied: As myosin moves via the biased Brownian motion, the entropic force acting on myosin exhibits an upward shift (i.e., a shift in the positive direction). Thus, the change in geometric features of myosin and the portion of F-actin near myosin, shift of the entropic force, and movement of myosin are strongly coupled. This view seems to be similar to that proposed by Terada *et al.*[15] although their physical interpretation is different from ours emphasizing the water-entropy effect.

The outline of the unidirectional movement can be described by the physical picture illustrated in Fig. 3, pending further analyses accounting for the details discussed above which *enhance* the unidirectional property of the movement (i.e., which expands the distance by which myosin can move on the average in one cycle). The directed movement is realized by repeated switches from one of the potential fields to the other. Similar pictures[8,10,4,11,12,14–16] have already been suggested. However, in some of them, the potential curves are drawn simply as the input and their physical origins are rather ambiguous. In the others, the physical explanations on the curves are given but they are not relevant to the water-entropy effect considered here. In the present work, the basic characteristics of the curves are qualitatively reproduced using an elaborate statistical-mechanical method with a firm physical basis emphasizing the water-entropy effect. (In Sec. IV C, we argue how the change from curve 1 to curve 2 is provided by the water-entropy effect.) Our picture is thus different from the previously suggested models. The picture is consistent with the experimental evidence that the binding of myosin to F-actin is entropically driven.[21–23]

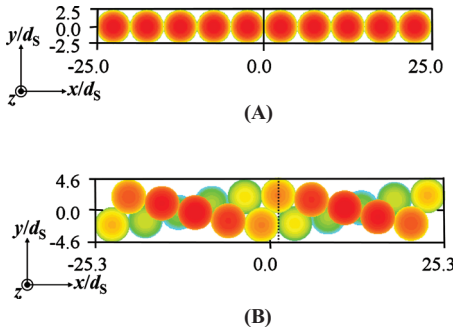

FIG. 4. Two models considered for the filament: One-dimensionally connected large hard spheres (a) and double helical structure formed by two sets of connected large hard spheres (b). The dotted line indicates $x/d_S=1.2$ (see Fig. 10). The position of an element sphere becomes farther from us as the color approaches blue, and the position becomes closer to us as the color approaches red.

III. MODEL AND THEORY

A. Model

We start with simple models accounting for only overall shapes of the protein and the filament as their geometric features. Our major concern is to analyze the spatial distribution of the entropic potential between a large solute and a large body immersed in small spheres with diameter d_S forming the solvent. ATP, Pi, and ADP are not considered because their concentrations are significantly small. The solute and the body correspond to a head of myosin and F-actin, respectively. The solute is modeled as a large hard sphere with diameter d_B. (We also consider large, aspherical solutes to examine the effects of geometric features of the solute: see Sec. IV C for more details.) As the body two model filaments are considered, model 1 is a set of one-dimensionally connected large hard spheres (i.e., unit spheres) with diameter d_G [Fig. 4(a)] and model 2 is a double helical structure formed by two sets of connected large hard spheres with diameter d_G [Fig. 4(b)]. The numbers of the unit spheres are 10 and 20 in models 1 and 2, respectively. The unit sphere corresponds to G-actin. Model 2 is more realistic than model 1 as a simplified model of F-actin. The neighboring unit spheres are in contact with one another, and there are no overlaps. In the present study, d_B and d_G are set at $5d_S$. Setting d_B and d_G at realistically large values ($\sim 20d_S$) (Refs. 18, 19, and 60) gives rise to unacceptably large computer-storage requirements. However, the qualitative aspects of our physical picture of the unidirectional movement are not likely to be altered because $5d_S$ is large enough to provide useful information on the entropic potential as evidenced in earlier works.[24,29,30,38,47]

B. Three-dimensional integral equation theory

Solute i of arbitrary geometry is immersed at infinite dilution in small spheres with diameter d_S forming the solvent. The Ornstein–Zernike (OZ) equation in the Fourier space[24,30,44,47,50–52] is expressed by

$$W_{iS}(k_x,k_y,k_z) = \rho_S C_{iS}(k_x,k_y,k_z) H_{SS}(k) \tag{1}$$

and the hypernetted-chain (HNC) closure equation[24,30,44,47,50–52] is written as

$$c_{iS}(x,y,z) = \exp\{-u_{iS}(x,y,z)/(k_B T)\}\exp\{w_{iS}(x,y,z)\} - w_{iS}(x,y,z) - 1. \tag{2}$$

Here, the subscript "S" denotes the solvent, $w=h-c$, c is the direct correlation function, h is the total correlation function, u is the potential, ρ is the bulk density, k_B is Boltzmann's constant, and T is the absolute temperature. The values of d_S and ρ_S are set at those of water under the normal condition: $\rho_S d_S^3 = 0.7317$. The capital letters (C, H, and W) represent the Fourier transforms. $H_{SS}(k)$ ($k^2 = k_x^2 + k_y^2 + k_z^2$) calculated using the radial-symmetric HNC theory for spherical particles is part of the input data. We emphasize that the OZ equation is *exact*.[36,44,47] On the other hand, the bridge function is neglected in the HNC closure equation. However, it has been verified that the 3D-OZ-HNC theory gives quantitatively reliable results.[24,29,30]

The numerical procedure is briefly summarized as follows: (1) $u_{iS}(x,y,z)$ is calculated at each 3D grid point, (2) $w_{iS}(x,y,z)$ is initialized to zero, (3) $c_{iS}(x,y,z)$ is calculated from Eq. (2), and $c_{iS}(x,y,z)$ is transformed to $C_{iS}(k_x,k_y,k_z)$ using the 3D fast Fourier transform (3D-FFT), (4) $W_{iS}(k_x,k_y,k_z)$ is calculated from Eq. (1), and $W_{iS}(k_x,k_y,k_z)$ is inverted to $w_{iS}(x,y,z)$ using the 3D-FFT, and (5) steps (3) and (4) are repeated until the input and output functions for $w_{iS}(x,y,z)$ become identical within convergence tolerance. On grid points where a solvent particle and the solute overlap, $\exp\{-u_{iS}(x,y,z)/(k_B T)\}$ is zero. On those where a solvent particle is in contact with the solute, it is set at 0.5, and otherwise it is unity. The grid spacing (Δx, Δy, and Δz) is set at $0.1 d_S$, and the grid resolution ($N_x \times N_y \times N_z$) is $1024 \times 512 \times 512$. It has been verified that the spacing is sufficiently small and the box size ($N_x \Delta x, N_y \Delta y, N_z \Delta z$) is large enough for the correlation functions at the box surfaces to be essentially zero.[30,47]

We consider solutes 1 and 2. Solute 1 is a large body, the filament illustrated in Fig. 4(a) or Fig. 4(b). Solute 2 is a large sphere with diameter d_B. First, the solute 1-solvent correlation functions [the Fourier transform of the direct correlation function is denoted by $C_{1S}(k_x,k_y,k_z)$] are calculated by following the procedure described above ($i=1$). Second, the solute 2-solvent correlation functions [the Fourier transform of the total correlation function is denoted by $H_{2S}(k)$] are calculated using the radial-symmetric HNC theory for spherical particles. The entropic potential between solutes 1 and 2 is described by the potential of mean force by assuming that the solvent particles are always in equilibrium with each configuration of the two solutes. This assumption is justified because in the real system the hydration structure steadies in picoseconds, while the movement of myosin occurs in milliseconds.[15] Hereafter, solutes 1 and 2 are referred to as "filament" and "large solute," respectively.

The potential of mean force between the two solutes $\Phi_{12}(x,y,z)$ are then obtained from

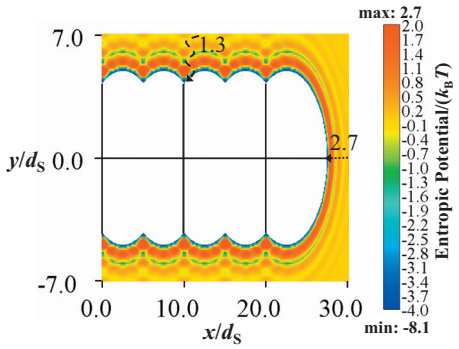

FIG. 5. Distribution of the entropic potential field formed for the large spherical solute near the filament on the cross section expressed by $z=0$ in model 1. The potential becomes lower as the color approaches thick blue, and the potential becomes higher as the color approaches thick red. The numbers given are scaled by $k_B T$. The maximum and minimum values of the potential scaled by $k_B T$ are also given. The center of the large solute cannot enter the domain drawn in white.

$$\Phi_{12}(x,y,z)/(k_B T) = u_{12}(x,y,z)/(k_B T) - w_{12}(x,y,z), \tag{3}$$

where $w_{12}(x,y,z)$ is calculated by inverting $W_{12}(k_x,k_y,k_z)$ given by

$$W_{12}(k_x,k_y,k_z) = \rho_S C_{1S}(k_x,k_y,k_z) H_{2S}(k). \tag{4}$$

The values of Φ_{12} which are not on the grid points are estimated using the linear interpolation.

The physical meaning of $\Phi_{12}(x,y,z)$ can be understood from

$$\Phi_{12}(x,y,z) = F(x,y,z) - F(\infty,\infty,\infty) \tag{5}$$

and

$$g_{12}(x,y,z) = \exp\{-\Phi_{12}(x,y,z)/(k_B T)\}, g_{12}(\infty,\infty,\infty) = 1. \tag{6}$$

Here, the x-, y-, and z-axes are taken and the origin of the coordinate system is chosen as illustrated in Fig. 4(a) or Fig. 4(b), $F(x,y,z)$ is the free energy of the solvent in the case where the large solute is at the position (x,y,z), and $g_{12}(x,y,z)$ the pair distribution function.

Due to the hard-body models, all the accessible system configurations share the same energy and the behavior of $\Phi_{12}(x,y,z)$ is purely entropic in origin. Hereafter, $\Phi_{12}(x,y,z)$ is referred to as the entropic potential. $-\partial\Phi_{12}(x,y,z)/\partial x$, for example, represents the entropic force in the x-direction. A great advantage of the 3D integral equation theory is that the spatial distribution of Φ_{12} is obtained from only a single calculation,[24,30] which is in marked contrast with the usual computer simulation.

IV. RESULTS AND DISCUSSION

A. Entropic potential formed in model 1

The large solute considered in this section is spherical. The distribution of the entropic potential on the cross section expressed by $z=0$ is shown in Fig. 5. It is apparent that the solute is strongly confined within a narrow space in contact with the filament. There are routes through which the solute can come in contact with the filament from the bulk (e.g., the route indicated by the broken line with the highest free-

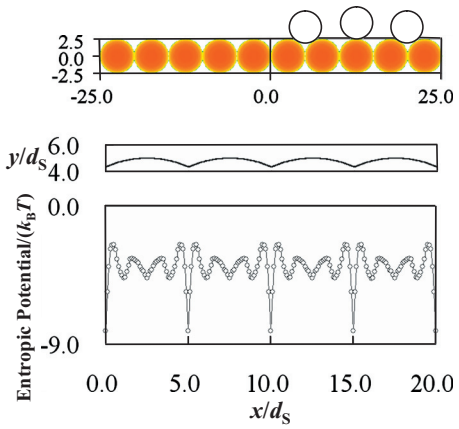

FIG. 6. Potential curve (bottom) formed for the large spherical solute along the trajectory where it is always in contact with the filament of model 1 (top). The y-coordinate of the center of the solute along the trajectory is also shown (middle).

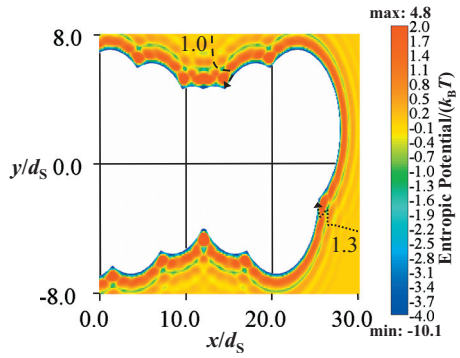

FIG. 8. Distribution of the entropic potential field formed for the large spherical solute near the filament on the cross section expressed by $z=0$ in model 2. The potential becomes lower as the color approaches thick blue, and the potential becomes higher as the color approaches thick red. The numbers given are scaled by k_BT. The maximum and minimum values of the potential scaled by k_BT are also given. The center of the large solute cannot enter the domain drawn in white.

energy barrier of $\sim 1.3k_BT$). However, once the solute enters the narrow space, it cannot be released to the bulk because the barrier in the opposite direction is much higher.

Figure 6 shows the potential curve formed for the large solute along the trajectory where it is always in contact with the filament. There are locations with sharply, deep local potential minima where the solute is in contact with two unit spheres of the filament. The distance between two adjacent locations equals the unit-sphere diameter d_G. The solute is trapped on these locations and can hardly move. Hence, the locations can be identified as the rigor binding sites for myosin on F-actin. When the solute is entropically bound to a rigor binding site, the free energy of the solvent decreases to a large extent (by $\sim 8.1k_BT$).

The distribution of the entropic potential on the cross section expressed by $x=0$ is shown in Fig. 7. There is a spherical shell within which the potential is negative and quite large, and the large solute can freely rotate around the long axis. Namely, the deep local potential minima mentioned above form a ringlike domain. Again, it is observed that the solute cannot escape from the narrow space in contact with the filament due to a high free-energy barrier.

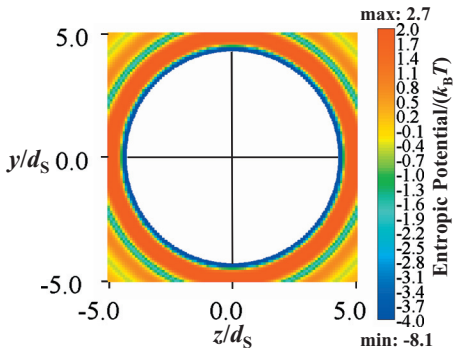

FIG. 7. Distribution of the entropic potential field formed for the large spherical solute near the filament on the cross section expressed by $x=0$ in model 1. The potential becomes lower as the color approaches thick blue, and the potential becomes higher as the color approaches thick red. The maximum and minimum values of the potential scaled by k_BT are also given. The center of the large solute cannot enter the domain drawn in white.

B. Entropic potential formed in model 2

The large solute considered in this section is spherical. The distribution of the entropic potential on the cross section expressed by $z=0$ is shown in Fig. 8. Although the distribution is more complicated than that in Fig. 5, it exhibits qualitatively the same feature: The solute is strongly confined within a narrow space in contact with the filament. There are routes through which the solute can come in contact with the filament from the bulk (e.g., the routes indicated by the broken line and by the dotted line with the highest free-energy barriers of $\sim 1.0k_BT$ and $\sim 1.3k_BT$, respectively). Model 2 provides more such routes than model 1. However, once the solute enters the narrow space, it cannot be released to the bulk because the barrier in the opposite direction is much higher.

Figure 9 shows the potential curve formed for the large solute along the trajectory where it is always in contact with a set of connected unit spheres in harmony with the helical

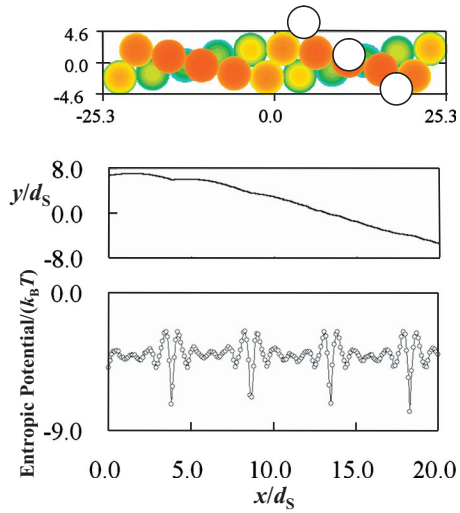

FIG. 9. Potential curve (bottom) formed for the large spherical solute along the trajectory where it is always in contact with a set of connected unit spheres in harmony with the helical structure in model 2 (top). The y-coordinate of the center of the solute along the trajectory is also shown (middle).

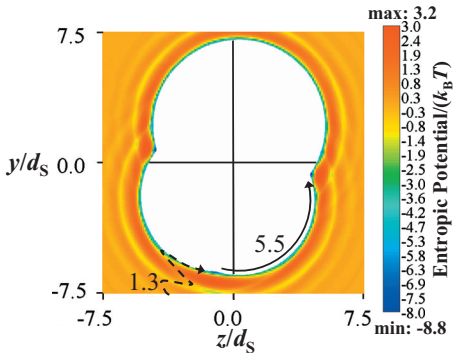

FIG. 10. Distribution of the entropic potential field formed for the large spherical solute near the filament on the cross section expressed by $x=1.2d_S$ in model 2. The potential becomes lower as the color approaches thick blue, and the potential becomes higher as the color approaches thick red. The numbers given are scaled by k_BT. The maximum and minimum values of the potential scaled by k_BT are also given. The center of the large solute cannot enter the domain drawn in white.

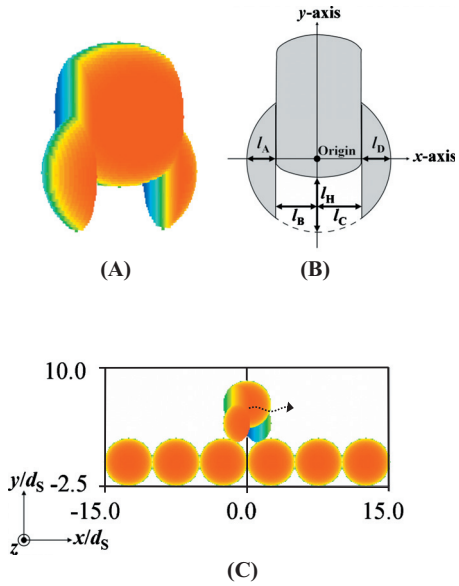

FIG. 11. Large aspherical solutes considered for mimicking myosin which is bound to F-actin only weakly. Three-dimensional visualization (a). Dimensions of the solutes (b). Solute A: $l_A=1.0d_S$, $l_B=1.5d_S$, $l_C=1.5d_S$, $l_D=1.0d_S$, and $l_H=2.0d_S$. Solute B: $l_A=0.9d_S$, $l_B=1.6d_S$, $l_C=1.4d_S$, $l_D=1.1d_S$, and $l_H=2.0d_S$. Solutes A and B are symmetrical and asymmetrical about the y-axis, respectively. Solute A on the filament (c). The position becomes farther from us as the color approaches blue, and the position becomes closer to us as the color approaches red. The dotted arrow indicates the trajectory.

structure. There are the locations with sharply deep local potential minima where the solute is in contact with two unit spheres of the filament. The distance between two adjacent locations is equal to the unit-sphere diameter d_G, although along the x-axis it is slightly smaller than d_G. The large solute is trapped on the locations and can hardly move. The locations can be identified as the rigor binding sites for myosin on F-actin.

Figure 10 shows the distributions of the entropic potential on the cross sections expressed by $x=1.2d_S$ [see Fig. 4(b)]. The large solute cannot rotate around the long axis due to the presence of high free-energy barriers. For example, the barrier of $\sim 5.5k_BT$ (this is the highest one) must be overcome for the route indicated by the solid line. Thus, the deep, local potential minima mentioned above form a pointlike domain. This is a clear difference between the results from models 1 and 2. Again, it is observed that the solute can come in contact with the filament from the bulk, for example, through the route indicated by the broken line whose highest barrier is $\sim 1.3k_BT$ (we note that the barrier in the opposite direction is much higher).

C. Effect of geometric features of large solute

On the basis of the results from models 1 and 2, we can conclude that the double helical structure of F-actin plays significant roles: There are more routes through which the solute can come in contact with the filament from the bulk, and the large solute cannot rotate around the long axis. However, curve 1 shown in Fig. 3 and the curves plotted in Figs. 6 and 9 share qualitatively the same characteristics: They are periodic and possess the sharp valleys with deep local potential minima on which the large solute is trapped. The basic characteristics of curve 1 have qualitatively been reproduced by our model calculations based on statistical mechanics. The remaining problem is the qualitative reproduction of curve 2.

As described in Sec. II, the essential characteristics required for curve 2 are the sufficiently high asymmetry for each period and smaller amplitudes in comparison to those of curve 1. A question then arises: How is the change from curve 1 to curve 2 provided? It is definite that the potential curve becomes asymmetrical for each period when the large solute and/or the unit sphere in the filament have aspherical shape. In the case of actomyosin, the large solute and the filament correspond to myosin and F-actin, respectively. In the present version of our physical picture, the shape of G-actin (the unit sphere in the filament) is assumed to remain virtually unchanged upon the ATP binding to myosin, and the change in the shape of myosin near the myosin/F-actin interface is the most important factor featuring curve 2. It is experimentally known that myosin with the ATP or ADP+Pi binding in states 2 and 3 has a cleft near the myosin/F-actin interface[5,6,57,58] (this cleft is closed in myosin without the binding in states 1, 4, and 5).

Here we present results of simple example calculations. With model 1 for the filament, two large aspherical solutes (solutes A and B) are considered as illustrated in Fig. 11. Solute A is symmetrical about the y-axis while solute B is asymmetrical. Each of the solutes has a cleft near the solute-filament interface, which is based on the experimental evidence[5,6,57,58] mentioned above. As observed in Fig. 11(c), when either of them contacts the filament, the decrease in the total excluded volume is smaller than in the case of the spherical large solute. That is, myosin is bound to F-actin only weakly. When the solute is aspherical, the calculation procedure for the entropic potential is more complex as explained in our earlier publication.[44] The orientation of the solute is fixed for simplification [see Fig. 11(c)]. Figure 12 shows the potential curve for one period formed for each of solutes A and B along the trajectory where it is always in contact with the filament. The curves in Figs. 12(a) and 12(b) are for solutes A and B, respectively. For the symmetrical

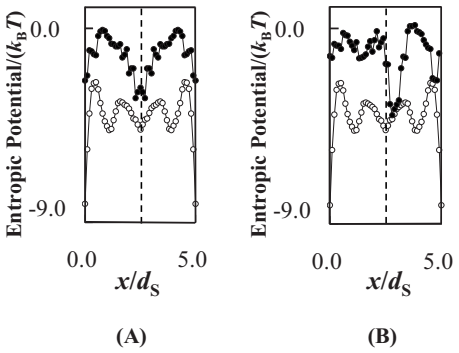

FIG. 12. Potential curve formed for each of the two large aspherical solutes shown illustrated in Fig. 11 along the trajectory where it is always in contact with the filament of model 1. The curves in (a) and (b) are for the large aspherical solutes A and B, respectively.

solute, the potential curve for one period is still symmetrical, but the amplitudes are smaller in comparison to those for the spherical solute. For the asymmetrical solute, the potential curve for one period is also asymmetrical, and the amplitudes are smaller in comparison to those for the spherical solute. The basic characteristics of curve 2 are qualitatively reproduced in Fig. 12(b).

In the real system, F-actin and myosin possess the polyatomic structures. When myosin is strongly bound to a rigor binding site of F-actin, their interface should be tightly packed. When ATP is bound to myosin, the structure of myosin undergoes a large change. As a result, the tight packing of the interfaces is lost, giving rise to the cleft. When the tight packing of myosin and ATP occurs, the packing of myosin and F-actin is inevitably loosened. The former should be more important for increasing the water entropy.

V. CONCLUDING REMARKS

We have described a new progress toward elucidating the mechanism of the unidirectional movement of a linear-motor protein along a filament by considering actomyosin as an example system. The new idea introduced is that, thanks to the entropic effect arising from the translational displacement of water molecules, the protein is confined within a narrow space in contact with the filament and the movement of the protein can be controlled by adjusting its geometric features. On the basis of the experimental observations known for a single myosin head (myosin subfragment 1: S1) and F-actin,[8,10,4,11,12] as well as the results of the present theoretical analyses, we have proposed the physical picture illustrated in Fig. 3 as the first step: The entropic potential field for the protein without the ATP or ADP+Pi binding to it is judiciously different from that for the protein with the binding, and the directed movement is realized by repeated switches from one of the fields to the other. This unidirectional property should be enhanced if we account for the following: (i) Myosin with the ATP binding in state 2, myosin with the ADP+Pi binding in state 3, and myosin with the ADP binding in state 4 (see Fig. 2) are more or less different in terms of geometric features;[5,6,57,58] (ii) the gradual change in geometric features of myosin and the portion of F-actin near myosin, shift of the entropic force acting on myosin, and movement of myosin are strongly coupled.

The qualitative aspects of curve 1 in Fig. 3 have been reproduced using the 3D integral equation theory combined with hard-body models. Myosin is strongly confined within a narrow space in contact with F-actin. Locations with sharply deep local potential minima, which correspond to the rigor binding sites for myosin on F-actin, are entropically formed. The minima occur when myosin is in contact with two G-actin molecules of the filament. Therefore, the distance between two adjacent rigor binding sites is equal to the size of G-actin. This result is in agreement with the experimental data.[8,10,4,11,12,60] The double helical structure of the filament considered in model 2 plays the following roles: There are more routes through which the solute can come in contact with the filament from the bulk, and the large solute cannot rotate around the long axis.

The physical factors causing the change in the entropic potential field from curve 1 to curve 2 in Fig. 3 have been argued with simple example calculations using the 3D integral equation theory. The potential curve formed for a large solute along a filament becomes asymmetrical when the asphericity is given to the solute shape. (In the real system myosin without the nucleotide binding is also aspherical,[5,6,57,58] giving rise to asymmetry of curve 1. However, as explained in Sec. II B, it is not important whether curve 1 is asymmetrical or not.) Upon the ATP binding to myosin, the overall shape of myosin becomes highly aspherical and at the same time a cleft is formed near the myosin/F-actin interface. Due to the cleft, the decrease in the total excluded volume for water molecules upon the contact of myosin to F-actin becomes smaller, leading to smaller differences between the potential minimum and maximum. In this way the potential curve possesses high asymmetry and smaller amplitudes for each period as curve 2.

The unidirectional movement in the real system could be accomplished by the interplay of multiple physical factors including previously suggested ones. To the best of our knowledge, this is the first time that the water-entropy effect is pointed out as an imperative factor missing in earlier works. Our concept is consistent with the experimental evidence that the binding of myosin to F-actin is entropically driven.[21–23] Further, an experimental measurement[23] has shown that the entropic gain upon the binding of myosin without the nucleotide to F-actin is as large as that upon the binding of myosin with ADP and much larger than that upon the binding of myosin with ATP. This is also in complete accord with curves 1 and 2 illustrated in Fig. 3.

In the real system, d_B/d_S and d_G/d_S are much larger than 5, the value considered in the present calculations. We note that the water-entropy effect becomes stronger with increasing d_B/d_S and/or d_G/d_S. The electrostatic interaction, which would be significantly strong in pure water, is largely screened by the counterions in aqueous solution under the physiological condition containing ~0.15M NaCl.[25] As a consequence, the water-entropy effect is expected to be dominantly large in comparison with the other effects. We have succeeded in elucidating the microscopic mechanisms of protein folding,[25,26,34,52,53,61] pressure,[25,26,35,62–64] heat,[26,65]

and cold[26,66,67] denaturating of proteins, and pressure-induced coil-helix transition of an alanine-based peptide[68] using our theoretical method wherein the water-entropy effect is treated as the key factor. The conventional view looking at only the water in the close vicinity of the protein surface is not capable of providing the success.

Our concept is consistent with the experimental result that the binding of myosin to F-actin is substantially weakened at low temperatures.[23] The reason is the following. We have recently elucidated the mechanism of cold denaturation of a protein.[26,66,67] Upon protein folding, the total volume available to the translational displacement of water molecules becomes larger, leading to an increase in the number of accessible configurations of water and the water entropy. This effect driving a protein to fold has been shown to become considerably less powerful at low temperatures, causing the denaturation. Likewise, upon the binding of myosin to F-actin, the total volume available to the translational displacement of water molecules becomes larger, leading to an increase in the water entropy. As in the case of cold denaturation, the effect driving myosin to bind to F-actin becomes considerably less powerful at low temperatures, which weakens the binding.

It is often emphasized that the electrostatic attractive interaction plays an essential role in the binding of myosin to F-actin.[16,20] However, before the binding the charged groups of myosin and of F-actin are stabilized in water by the electrostatic attractive interactions *with water molecules*. Such stabilization is lost upon the binding. This loss, which is usually referred to as the dehydration penalty, can be even larger. In fact, it is experimentally known that the binding accompanies a positive change in enthalpy.[21–23]

The polyatomic structures of myosin and F-actin are not taken into consideration in the present study. Nevertheless, a significant amount of interesting information is revealed using the 3D integral equation theory combined with simple models focusing the overall shapes alone: The present study sheds new light on the mechanism of the unidirectional movement of a linear-motor protein along a filament. In the near future, we intend to move on the analyses pursuing the issue described in Sec. II C, accounting for the polyatomic structures of myosin and F-actin, and allowing myosin to change its orientation when the potential curve is drawn. In such studies treating myosin and F-actin with polyatomic structures and realistic sizes, our hybrid[34,35,49,53,64–70] of the integral equation theory and the morphometric approach[71,72] is expectedly a practical tool. The effects of the enthalpic component of the solvation of solutes are also to be examined.

ACKNOWLEDGMENTS

This work was supported by Grants-in-Aid for Scientific Research on Innovative Areas (Nos. 20118004, 20118008, and 20118009) from the Ministry of Education, Culture, Sports, Science and Technology of Japan, by the Grand Challenges in Next-Generation Integrated Nanoscience, MEXT, Japan, and by Kyoto University Global Center of Excellence (GCOE) of Energy Science.

[1] S. M. Block, Biophys. J. **92**, 2986 (2007).
[2] E. Hirakawa, H. Higuchi, and Y. Y. Toyoshima, Proc. Natl. Acad. Sci. U.S.A. **97**, 2533 (2000).
[3] J. L. Ross, M. Y. Ali, and D. M. Warshaw, Curr. Opin. Cell Biol. **20**, 41 (2008).
[4] T. Yanagida, S. Esaki, A. H. Iwane, Y. Inoue, A. Ishijima, K. Kitamura, H. Tanaka, and M. Tokunaga, Philos. Trans. R. Soc. London, Ser. B **355**, 441 (2000).
[5] A. Houdusse and H. L. Sweeney, Curr. Opin. Cell Biol. **11**, 182 (2001).
[6] P. Coureux, H. L. Sweeney, and A. Houdusse, EMBO J. **23**, 4527 (2004).
[7] T. M. Watanabe, H. Tanaka, A. H. Iwane, S. Yonekura, K. Homma, A. Inoue, R. Ikebe, T. Yanagida, and M. Ikebe, Proc. Natl. Acad. Sci. U.S.A. **101**, 9630 (2004).
[8] T. Okada, H. Tanaka, A. H. Iwane, K. Kitamura, M. Ikebe, and T. Yanagida, Biochem. Biophys. Res. Commun. **354**, 379 (2007).
[9] Y. Okada and N. Hirokawa, Science **283**, 1152 (1999).
[10] K. Kitamura, M. Tokunaga, A. H. Iwane, and T. Yanagida, Nature (London) **397**, 129 (1999).
[11] K. Kitamura, M. Tokunaga, S. Esaki, A. H. Iwane, and T. Yanagida, Biophysics (Engl. Transl.) **1**, 1 (2005).
[12] T. Yanagida, M. Iwaki, and Y. Ishii, Philos. Trans. R. Soc. London, Ser. B **363**, 2123 (2008).
[13] R. Cooke, Physiol. Rev. **77**, 671 (1997).
[14] F. Jülicher, A. Ajdari, and J. Prost, Rev. Mod. Phys. **69**, 1269 (1997).
[15] T. P. Terada, M. Sasai, and T. Yomo, Proc. Natl. Acad. Sci. U.S.A. **99**, 9202 (2002).
[16] M. Takano, T. P. Terada, and M. Sasai, Proc. Natl. Acad. Sci. U.S.A. **107**, 7769 (2010).
[17] S. Sporer, C. Goll, and K. Mecke, Phys. Rev. E **78**, 011917 (2008).
[18] Y. Cong, M. Topf, A. Sali, P. Matsudaira, M. Dougherty, W. Chiu, and M. F. Schmid, J. Mol. Biol. **375**, 331 (2008).
[19] S. Mouilleron, S. Guettler, C. A. Langer, R. Treisman, and N. Q. McDonald, EMBO J. **27**, 3198 (2008).
[20] Y. Liu, M. Scolari, W. Im, and H. Woo, Proteins **64**, 156 (2006).
[21] S. Highsmith, Arch. Biochem. Biophys. **180**, 404 (1977) (the author incorrectly claimed that the major factor for the binding of myosin to F-actin is the electrostatic attractive interaction).
[22] T. Kodama, Physiol. Rev. **65**, 467 (1985).
[23] T. Katoh and F. Morita, J. Biochem. (Tokyo) **120**, 189 (1996).
[24] M. Kinoshita, Chem. Eng. Sci. **61**, 2150 (2006).
[25] M. Kinoshita, Front. Biosci. **14**, 3419 (2009).
[26] M. Kinoshita, Int. J. Mol. Sci. **10**, 1064 (2009).
[27] S. Asakura and F. Oosawa, J. Chem. Phys. **22**, 1255 (1954).
[28] S. Asakura and F. Oosawa, J. Polym. Sci. **33**, 183 (1958).
[29] M. Kinoshita and T. Oguni, Chem. Phys. Lett. **351**, 79 (2002).
[30] M. Kinoshita, J. Chem. Phys. **116**, 3493 (2002).
[31] P. Bryk, R. Roth, M. Schoen, and S. Dietrich, Europhys. Lett. **63**, 233 (2003).
[32] A. D. Dinsmore, A. G. Yodh, and D. J. Pine, Nature (London) **383**, 239 (1996).
[33] M. Kinoshita, J. Chem. Phys. **128**, 024507 (2008).
[34] T. Yoshidome, M. Kinoshita, S. Hirota, N. Baden, and M. Terazima, J. Chem. Phys. **128**, 225104 (2008).
[35] Y. Harano, T. Yoshidome, and M. Kinoshita, J. Chem. Phys. **129**, 145103 (2008).
[36] P. Attard and G. N. Patey, J. Chem. Phys. **92**, 4970 (1990).
[37] T. Biben, P. Bladon, and D. Frenkel, J. Phys.: Condens. Matter **8**, 10799 (1996).
[38] M. Kinoshita, S. Iba, K. Kuwamoto, and M. Harada, J. Chem. Phys. **105**, 7177 (1996).
[39] R. Dickman, P. Attard, and V. Simonian, J. Chem. Phys. **107**, 205 (1997).
[40] B. Götzelmann, R. Evans, and S. Dietrich, Phys. Rev. E **57**, 6785 (1998).
[41] R. Roth, B. Götzelmann, and S. Dietrich, Phys. Rev. Lett. **83**, 448 (1999).
[42] R. Roth, R. Evans, and S. Dietrich, Phys. Rev. E **62**, 5360 (2000).
[43] R. Roth, R. van Roji, D. Andrienko, K. R. Mecke, and S. Dietrich, Phys. Rev. Lett. **89**, 088301 (2002).
[44] M. Kinoshita, Chem. Phys. Lett. **387**, 47 (2004).
[45] M. Kinoshita, Chem. Phys. Lett. **387**, 54 (2004).
[46] P.-M. König, R. Roth, and S. Dietrich, Europhys. Lett. **84**, 68006 (2008).
[47] K. Amano and M. Kinoshita, Chem. Phys. Lett. **488**, 1 (2010).
[48] W. Kauzmann, Adv. Protein Chem. **14**, 1 (1959).
[49] T. Yoshidome, K. Oda, Y. Harano, R. Roth, Y. Sugita, M. Ikeguchi, and M. Kinoshita, Proteins **77**, 950 (2009).

[50] D. Beglov and B. Roux, J. Chem. Phys. **103**, 360 (1995).
[51] M. Ikeguchi and J. Doi, J. Chem. Phys. **103**, 5011 (1995).
[52] Y. Harano and M. Kinoshita, Biophys. J. **89**, 2701 (2005).
[53] S. Yasuda, T. Yoshidome, H. Oshima, R. Kodama, Y. Harano, and M. Kinoshita, J. Chem. Phys. **132**, 065105 (2010).
[54] H. Iwamoto, K. Oiwa, T. Suzuki, and T. Fujisawa, J. Mol. Biol. **305**, 863 (2001).
[55] J. Sakamaki, H. Honda, E. Imai, K. Hatori, K. Shimada, and K. Matsuno, Biophys. Chem. **105**, 59 (2003).
[56] K. Hatori, J. Sakamaki, H. Honda, K. Shimada, and K. Matsuno, Biophys. Chem. **107**, 283 (2004).
[57] A. Houdusse, V. N. Kalabokis, D. Himmel, G. Szent-Gyorgyi, and C. Cohen, Cell **97**, 459 (1999).
[58] P. Coureux, A. L. Wells, J. Menetrey, C. M. Yengo, C. A. Morris, H. L. Sweeney, and A. Houdusse, Nature (London) **425**, 419 (2003).
[59] M. S. P. Siddique, G. Mogami, T. Miyazaki, E. Katayama, T. Q. P. Uyeda, and M. Suzuki, Biochem. Biophys. Res. Commun. **337**, 1185 (2005).
[60] L. F. Chen, H. Winkler, M. K. Reedy, M. C. Reedy, and K. A. Taylor, J. Struct. Biol. **138**, 92 (2002).
[61] Y. Harano and M. Kinoshita, Chem. Phys. Lett. **399**, 342 (2004).
[62] Y. Harano and M. Kinoshita, J. Phys.: Condens. Matter **18**, L107 (2006).
[63] Y. Harano and M. Kinoshita, J. Chem. Phys. **125**, 024910 (2006).
[64] T. Yoshidome, Y. Harano, and M. Kinoshita, Phys. Rev. E **79**, 011912 (2009).
[65] K. Amano, T. Yoshidome, Y. Harano, K. Oda, and M. Kinoshita, Chem. Phys. Lett. **474**, 190 (2009).
[66] T. Yoshidome and M. Kinoshita, Phys. Rev. E **79**, 030905(R) (2009).
[67] H. Oshima, T. Yoshidome, K. Amano, and M. Kinoshita, J. Chem. Phys. **131**, 205102 (2009).
[68] T. Yoshidome and M. Kinoshita, Chem. Phys. Lett. **477**, 211 (2009).
[69] Y. Harano, R. Roth, and M. Kinoshita, Chem. Phys. Lett. **432**, 275 (2006).
[70] Y. Harano, R. Roth, Y. Sugita, M. Ikeguchi, and M. Kinoshita, Chem. Phys. Lett. **437**, 112 (2007).
[71] P. M. König, R. Roth, and K. R. Mecke, Phys. Rev. Lett. **93**, 160601 (2004).
[72] R. Roth, Y. Harano, and M. Kinoshita, Phys. Rev. Lett. **97**, 078101 (2006).